Mon. Not. R. astr. Soc. (1986) **219**, 225–239

Study of quiescent state X-ray emission from flare stars

P. C. Agrawal,* A. R. Rao and B. V. Sreekantan *Tata Institute of Fundamental Research, Homi Bhabha Road, Colaba, Bombay 400 005, India*

Accepted 1985 August 22. Received 1985 August 21; in original form 1985 May 29

Summary. Results on the X-ray emission from flare stars observed with the imaging proportional counter (IPC) on the *Einstein Observatory* are described. The mean value of the quiescent state X-ray luminosity L_x of the seven detected flare stars is found to be $\sim 2\times10^{28}$ erg s^{-1}. Analysis of the energy spectra of three of the stars gives the value of the corona temperature as 3×10^6 K. Results on gradual flux variations by a factor of ~ 2 in G 735 and the occurrence of a short duration ($\simeq 400$ s) flare in G 729 are presented. A study of the distribution of the ratio of the X-ray luminosity to the bolometric luminosity (L_x/L_{Bol}) for all the X-ray-observed flaring and non-flaring dwarf M stars shows that the L_x/L_{Bol} distribution of the flare stars is remarkably similar to that of the regular period RS CVn binaries but dissimilar to that of the non-flaring dwarf M stars. A strong correlation is found between L_x and L_{Bol} for the flare stars and regular period RS CVn binaries described by $L_x = 10^{-3.23\pm0.22} L_{Bol}$. The correlation between L_x and the luminosities of chromospheric and transition region lines in flare stars is also discussed. No compelling evidence is found for a dependence of L_x/L_{Bol} (or L_x) on the rotation velocity or rotation period for the limited sample of flare stars with available data. Finally similarities between the X-ray spectra of the flare stars and those of the RS CVn binaries are discussed.

1 Introduction

Flare stars are a group of dwarf red stars, generally of spectral type M, which exhibit intense flaring activity in the optical band. Flares in the radio, ultraviolet and X-ray bands have also been detected from several flare stars in recent years. These stars are characterized by their strong chromospheric activity as indicated by the presence of emission lines of hydrogen (H_α) and Ca II in their optical spectra and emission lines of Mg II, O I, Si II etc. in their ultraviolet spectra which are present even during the quiescent state. High fluxes of high temperature transition region lines such as N V, C IV, He II etc. have been detected with the *IUE* from several flare stars in their quiescent state. Surface fluxes of these transition region lines are one to two orders of magnitude higher than those of the quiet Sun which indicates their extremely active nature.

* Guest investigator with the *Einstein Observatory*.

About 80 flare stars, all lying within 25 pc of the Sun, have been detected so far. All these stars, with the exception of two, namely G 229 and Ross 128 (G 447), are hydrogen emission line stars. Except for four stars which are of spectral type K, the rest are dM stars. A large number of these stars are in binaries, usually of visual or astrometric type, in which both components of the binary are flare stars. Regular period photometric variations, usually referred to as 'BY Draco variability', have also been detected in a number of flare stars. This is attributed to the presence of large-scale star spots on the photospheres of the stars and the rotation of the stars results in light variations due to the change in the number of viewed spots. For a review of the optical characteristics of the flare stars refer to Kunkel (1975). A detailed discussion of the various physical parameters of the flare stars has been given by Pettersen (1980).

First detection of X-ray emission from the flare stars was reported by Heise *et al.* (1975) when they observed an X-ray flare from YZ CMi and a coincident X-ray and optical flare from UV Ceti with the *ANS* satellite. Observations with *HEAO-1* revealed X-ray flaring in AT Mic (Kahn *et al.* 1979) and a major X-ray flare event was detected by Haisch *et al.* (1983) in the nearest flare star Proxima Cen. Thus X-ray flaring seems to be a common feature of the flare stars. Reports of the quiescent state X-ray emission from the flare stars, however, came from the *Einstein* stellar survey (Vaiana *et al.* 1981). Several nearby flare stars were detected in this survey with their X-ray luminosity L_x in the range 10^{27}–10^{29} erg s^{-1}. Following this discovery we carried out a survey of flare stars with the imaging proportional counter (IPC) on the *Einstein Observatory* (*EO*) under the guest investigation programme of NASA to study the quiescent state X-ray emission of flare stars and to detect any correlation between their chromospheric, transition region and coronal emissions. Preliminary results were reported at the *IAU Colloquium No. 71* (Agrawal *et al.* 1983). In this paper we report detailed results of the survey. We also present in list form a summary of the X-ray properties of all the detected flare stars as well as other dMe and dM stars. We compare the X-ray characteristics of the flare stars with those of the non-flaring dMe and dM stars and point out similarities in X-ray emission characteristics of the flare stars with those of the RS CVn binaries. Next we discuss the correlation between L_x and bolometric luminosity L_{Bol} as well as between L_x and luminosities in chromospheric and transition region lines. We also discuss the dependence of L_x on the rotation periods of the flare stars. Finally, we briefly discuss similarities between the spectra of the flare stars and those of the RS CVn binaries.

2 Observations and results

The observation programme included 12 flare stars from the list of Kunkel (1975), which were not included in any other surveys. Only seven of these stars could be observed, however, before *EO* ceased operation. A summary of the optical parameters of these stars is given in Table 1. All are single UV Ceti-type flare stars except for G 493.1 (FN Vir) which is a spectrosopic binary. Five of

Table 1. Summary of X-ray results on flare stars surveyed in this work.

Gliese no.	Other name	Spectral type	m_v	Distance (pc)	Effective exposure time (s)	IPC count rate (count s^{-1} × 10^{-2})	Log L_x (erg s^{-1})	Log $\frac{L_x}{L_{Bol}}$
229	BD−21°1377	dM2.5	8.13	5.7	10500	1.07±0.22	26.9	−5.35
–	PZ Mon	dK2e	10.8	16	5343	2.10±0.35	28.1	−3.60
398	L113−55	dM4e	12.61	13.7	1426	7.42±0.86	28.5	−3.13
493.1	FN Vir	dM5e	13.34	11.1	1282	2.54±0.69	27.9	−3.49
729	V1216 Sgr	dM4.5e	10.60	2.9	3676	22.8±0.90	27.7	−3.66
735	V1285 Aql	dM3e	10.07	10.9	7518	26.7±0.60	28.9	−3.26
791.2	HU Del	dM6e	13.06	9.4	5265	6.32±0.45	28.1	−3.22

the seven surveyed stars are dMe stars, one star (G 229) is classified as a dM star and one star (PZ Mon) is of spectral type dK2e. The IPC exposure times of these stars ranged from about 10^3 to 10^4 s. X-ray emission was detected from all the seven stars. The exposure times and observed IPC count rates are shown in Table 1. Two of the stars were relatively bright X-ray sources with IPC count rates of ~ 0.2 counts s^{-1}.

2.1 X-RAY LUMINOSITIES

To convert the observed count rates to flux values we need to know the X-ray spectra of the stars. Spectral analysis of the IPC pulse height data was carried out for three of the stars having more than 250 source counts. This analysis, discussed in detail in the next section, yielded flux conversion factors in the range $(1.39–1.51)\times 10^{-11}$ erg per IPC count. In the *Einstein* stellar survey of Vaiana *et al.* (1981) and the survey of nearby stars by Johnson (1981), a flux conversion factor of 2×10^{-11} erg per IPC count, appropriate for thermal emission from a plasma at a temperature of 10^7 K, was used. We have therefore also chosen the same conversion factor to facilitate comparison of our data with those for the other flare stars included in various other surveys. Using distance values derived from parallax measurements given by Gliese (1969) we computed L_x values which are listed in Table 1. The star PZ Mon is not included in the Gliese catalogue and we therefore used the distance value given by Gurzadyan (1980) for computing its L_x. A search for time variability showed no evidence of flaring activity during our observations in any of the stars except G 729, in which a rather weak flare of $\simeq$400 s duration was detected and was excluded from the calculation of the average quiescent state counting rate of G 729. The observed L_x values therefore represent the quiescent state X-ray emission. Details of the X-ray flare in G 729 and the slow intensity variation observed in G 735 will be presented in a later section. The mean value of L_x for our sample of seven flare stars is 2×10^{28} erg s^{-1}.

Since L_x depends on the assumed size and distance of the star, a more appropriate quantity to measure the X-ray activity of a star is the ratio of its X-ray luminosity to its bolometric luminosity (L_x/L_{Bol}) which is independent of the size as well as the distance of the star. Using values of absolute magnitude (M_v) given by Kunkel (1975) and the following relation for bolometric correction (BC)

$$BC = -0.397\, M_v + 2.386$$

due to Pettersen (1983) we compute BC and M_{Bol} for all the stars. The L_{Bol} values were then computed using the relation

$$L_{Bol} = 3.02\times 10^{35}\times 10^{-0.4\, M_{Bol}} \text{ erg s}^{-1}$$

(Lang 1980).

Finally values of the ratio L_x/L_{Bol} were calculated and these are shown in the last column of Table 1. Notice that except for G 229, which is a dM star, L_x/L_{Bol} values for the other six stars lie within a rather narrow range of a factor of 3.4 with a mean value of 4.6×10^{-4}. It should be pointed out that there is a spread in the L_x values for these six stars by a factor of $\sim$16. For G 229 the L_x

Table 2. Summary of spectral parameters.

Star	Best fit kT (keV)	EM ($cm^{-3}\times 10^{50}$)	Reduced χ^2	Flux conversion factor (erg per IPC count$\times 10^{-11}$)
G 729	0.26	1.2	1.38	1.51
G 735	0.28	1.7	2.1	1.47
G 791.2	0.28	2.9	0.82	1.39

value is an order of magnitude lower and the L_x/L_{Bol} is two orders of magnitude lower than those for the other stars. However, as discussed later, these values are comparable with those observed for the non-flaring dM stars. It should be pointed out that the star G 229 exhibits rather weak flaring activity compared with the other flare stars (Kunkel 1973). The X-ray observations indicate that, at least in its quiescent state, G 229 resembles non-active dM stars rather than the active dMe flare stars.

2.2 X-RAY SPECTRA

The number of source counts with useful pulse height data exceeded 900 and 1850 for G 729 and 735 respectively and were about 280 for G 791.2. The spectral fitting was therefore tried for these three sources using the Raymond–Smith model (Raymond & Smith 1977, 1979, unpublished). The IPC gain appropriate for the day of observation of the sources, represented by the BAL parameter derived from inflight calibration, was used for spectral fitting for each source. Since these stars lie within 12 pc, the absorption of X-rays in the interstellar medium is negligible for them. Therefore $\log N_H = 18.0$ was used in the spectral fitting runs. This was independently verified for each source by allowing N_H to vary in a run and it was found that in each case the best fit was always obtained for the minimum value of N_H. The best-fit value of kT, the emission

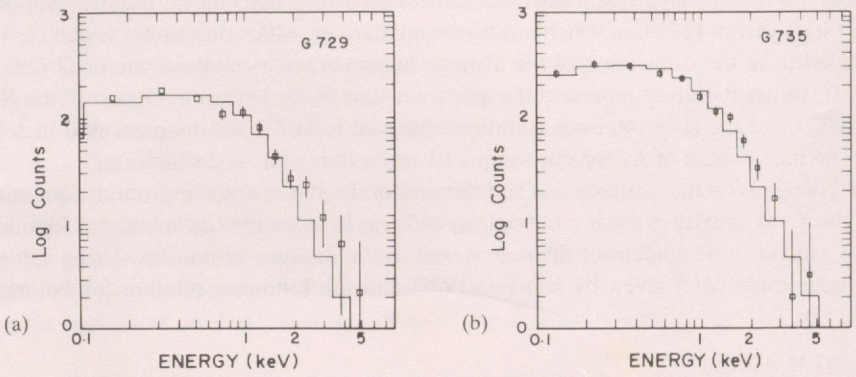

Figure 1. (a) The observed count spectrum of the flare star G 729. The histogram shows the best-fit Raymond–Smith spectrum with $kT = 0.26$ keV. (b) The observed count spectrum for the flare star G 735. The best-fit Raymond–Smith spectrum with $kT = 0.28$ keV is indicated by the histogram.

measure (EM) and the derived flux conversion factor are listed in Table 2. The best-fit spectra for G 729 and 735 are shown in Fig. 1(a) and (b), respectively. The kT values for the three sources are about the same but the emission measures differ by an order of magnitude. However, note that while acceptable spectral fits are obtained for G 791.2 and 729, the value of the reduced χ^2 shown in Table 2 is unacceptably high (corresponding to a probability of 0.02) for G 735. As seen in Fig. 1(b) this happens because the observed flux values above 1.5 keV lie systematically above the best-fit spectrum. This trend is also visible in the spectrum of G 729 in Fig. 1(a). There is thus a suggestion for the presence of a higher temperature component in the spectra of these two stars. Unfortunately the standard IPC spectral fitting programme has no provision for fitting a two-temperature Raymond–Smith model and therefore we cannot draw any inference about the high temperature component at this time. It may be pointed out, however, that Swank & Johnson (1982) required a two-temperature model to fit the spectrum of the flare star Wolf 630AB (G 644 AB) observed with the solid state spectrometer on the *EO*. The dominant low temperature

component had $kT=0.54$ keV and the temperature required for the hotter component was $kT \geqslant 0.7$ keV. The luminosity and emission measure of the high temperature component was only one-third of those for the low temperature component. The temperature of $\sim 3\times10^6$ K for the coronae of the three stars in our sample is in good agreement with the value of 3.5×10^6 K obtained by Haisch & Linsky (1980) for the flare star Proxima Cen.

2.3 TIME VARIATIONS OF THE X-RAY INTENSITY

A search for the intensity variations in the count rate versus time plots for the observed stars led to the detection of variability in two of the stars, namely G 729 and 735. A plot of the counts grouped in 100 s bins versus time is shown in Fig. 2 for G 729. There is clear indication of a small X-ray flare occurring at about 6 ks after the start of the observations. The time of commencement of the flare is 5.063 hr UT on 1981 March 24. The proposition that the count rate increase was due to the source was verified by checking the off-source background in the IPC image which was found to be constant during the observation of G 729. The rise time of the flare was less than 100 s and its decay time was ~300 s. The statistical significance of the excess counts detected during the flare is 4.7σ above the average quiescent state count rate of the source. The L_x value at the flare peak was $\sim 5\times10^{27}$ erg s^{-1} and the total energy released in the 0.1–4 keV band was $\sim 10^{30}$ erg. Similar minor X-ray flare events had been detected in the flare star YZ CMi by Kahler *et al.* (1982) and in G 644 AB by Johnson (1981). The short duration of the flare suggests a similarity to impulsive solar X-ray burst events. The rise and decay times of the observed X-ray flare are similar to those of the optical flares seen in G 729 (Cristaldi & Rodono 1973). The detection of one flare event in about 1 hr of observing time is not inconsistent with the reported flare frequency of ~0.15–0.35 flares per hour (Feix 1974; Jarrett & Grabner 1974).

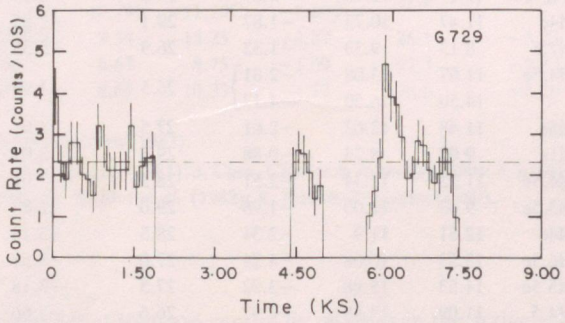

Figure 2. Plot of the IPC count rate versus time for the flare star G 729. The zero time corresponds to 3.396 hr UT on 1981 March 24. A weak X-ray flare is clearly seen at $T=6$ ks. The quiescent state count rate is indicated by the broken line in the figure.

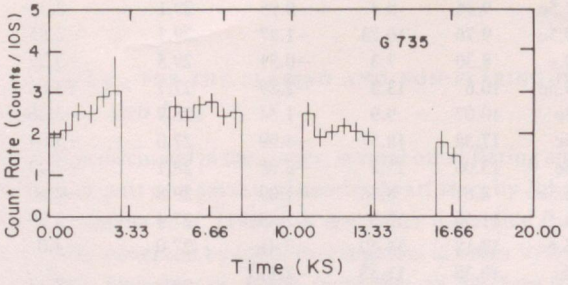

Figure 3. The X-ray light curve of the flare star G 735. Time $T=0.0$ corresponds to 6.188 hr UT on 1981 March 7.

The X-ray light curve of the star G 735, with counts grouped in 500-s time bins, is shown in Fig. 3. As can be seen there is at first a gradual increase in the count rate from 0.19 to 0.29 counts s^{-1} in less than an hour, at which level the count rate stays for about 2 hr. This is followed by a slow decline to a level of 0.16 counts s^{-1} in about 1.7 hr. Thus there is a change in the count rate by a factor of 1.8 in about 5 hr. A constant-intensity-source hypothesis gives an unacceptably high reduced χ^2 of 3.24. Constancy of the background during our observation of G 735 was verified by measurement of the background count rate in an off-source field in the IPC image. The reality of the intensity variations is therefore beyond doubt. This kind of slow variability could arise as a result of a change in the number of viewed X-ray active regions with the rotation of the star. This variablity may be the X-ray analogue of the BY Draco variability seen in the optical band in many flare stars. Another possible explanation may be that the observed variations are intrinsic to the active regions on the star. It may be mentioned that Linsky *et al.* (1982) detected variations in the flux of the transition region lines by 30–70 per cent from the flare star AT Mic over a time-scale of

Table 3. Summary of data on X-ray-observed flare stars and non-flaring dwarf M stars.

Gliese No.	Star name	Spectral type	m_v	M_v	BC	Log L_x (erg s^{-1})	Log (L_x/L_{Bol})	Reference for L_x	Comment (V in km s^{-1})*
(1)	(2)	(3)	(4)	(5)	(6)	(7)	(8)	(9)	(10)
(a) Flaring dMe and dM stars									
15A	DM+43.44	dM2.5	8.07	10.32	−1.71	27.2	−4.96	1	
15B	GQ And	dM4.5e	11.04	13.29	−2.89				
65A	L726−8	dM5.5e	12.45	15.35	−3.71	27.5	−3.59	2	
65B	UV Cet	dM6e	12.95	15.85	−3.91				
83.1	TZ Ari	dM8e	12.27	13.92	−3.14	27.6	−3.57	4	
166C	40 Eri C	sM4e	11.17	12.73	−2.67	28.3	−3.16	3	
206	Ross 42	dM4e	11.47	10.73	−1.87	29.1	−2.85	4	
229	BD−21°1377	dM2.5	8.13	9.33	−1.32	26.9	−5.35	5	No H_α emission
234A	Ross 614A	dM4.5e	11.07	13.08	−2.81	26.5	−4.96	6	
234B	Ross 614B	–	14.50	16.50	−4.17				
268	Ross 896	dM5e	11.48	12.62	−2.61	27.5	−4.01	6	
278C	YY Gem	dM1e	9.07	8.23	−0.88	29.5	−3.01	2, 7	SB2, V=38.5
285	YZ CMi	dM4.5e	11.23	12.34	−2.51	28.5	−3.01	8	V=5.5
388	AD Leo	dM3.5e	9.43	11.00	−1.98	29.0	−2.88	6	
398	L1113−55	dM4e	12.61	11.9	−2.34	28.5	−3.13	5	
406	CN Leo	dM6.5e	13.53	16.68	−4.24	27.0	−3.51	2	
412B	WX UMa	dM5.5e	14.53	15.88	−3.92	27.5	−3.18	1	
447	Ross 128	dM4.5	11.09	13.48	−2.97	26.6	−4.66	4	No H α emission
490A	DM+36.2322	dM1.5e	10.60	9.4	−1.35	29.0	−3.32	2	V=8.6
490B	G164−31	dM3.5e	13.16	11.9	−2.34				
493.1	FN Vir	dM5e	13.34	13.11	−2.82	27.9	−3.49	5	SB
551	Prox. Cen.	dM5e	11.05	15.45	−3.75	27.2	−3.62	9	
616.2	DM+55.1823	dM1.5e	9.96	8.4	−0.95	29.1	−3.39	6	
644AB	V1054 Oph	dM3.5e	9.76	10.73	−1.87	29.1	−2.85	1	
719	BY Dra	dM0.e	8.30	7.3	−0.51	29.5	−3.25	6	SB2, V=8.9
729	V1216 Sgr	dM4.5e	10.6	13.3	−2.89	27.7	−3.66	5	
735	V1285 Aql	dM3e	10.07	9.9	−1.54	28.9	−3.26	5	
752B	V1298 Aql	dM5e	17.38	18.57	−4.99	27.0	−3.04	2	
791.2	HU Del	dM6e	13.06	13.2	−2.85	28.1	−3.22	5	
803	AU Mic	dM2.5e	8.61	8.76	−1.09	29.8	−2.60	7	V=6.2
860B	DO Cep	dM4.5e	11.30	13.3	−2.89	27.4	−3.90	1	
866	L789−6	dM5.5e	12.18	14.60	−3.41	27.0	−4.0	4	
896A	DM+19.5116	dM4e	10.38	11.33	−2.11	28.8	−3.13	2	
896B	EQ Peg	dM5e	12.40	13.4	−2.93				

Table 3 –*continued*

Gliese No.	Star name	Spectral type	m_v	M_v	BC	Log L_x (erg s^{-1})	Log (L_x/L_{Bol})	Reference for L_x	Comment (V in km s^{-1})*
(1)	(2)	(3)	(4)	(5)	(6)	(7)	(8)	(9)	(10)
(b) dKe flare stars									
103	CC Eri	K7Ve	8.70	8.4	−0.84	29.4	−3.05	7	SB2, V=19.8
517	EQ Vir	dK5e	9.34	8.3	−0.60	29.4	−3.00	2	V=7.9
–	PZ Mon	dK2e	10.8	9.78	−0.35	28.1	−3.60	5	
(c) Non-flaring dMe stars									
213	Ross 47	dM4.1e	11.60	12.73	−2.66	27.2	−4.31	1	
783B	−36°13940	dM5e	11.50	12.7	−2.66	≤ 27.7	≤ −4.80	1, 4	
905	HH And	dM5.5e	12.29	14.80	−3.49	26.3	−4.59	4	
(d) Non-flaring dM stars									
191	Kapteyn	dM0	8.81	10.89	−1.94	≤ 26.5	≤ −5.36	4	
195A	ADS 3841H	dM2	10.2	9.6	−1.43	27.9	−4.37	4	
195B	Yale 1193	dM5	13.7	13.1	−2.82				
402	Wolf 358	dM5	11.66	12.42	−2.55	≤ 26.9	≤ −4.61	4	
445	Yale 2722	dM4	10.92	12.38	−2.54	≤ 26.7	≤ −4.84	1	
461	BD+1°2684	dM2	10.2	9.1	−1.23	28.2	−4.13	4	
–	Ross 476	dM6	14.34	12.7	−2.66	28.0	−3.46	4	
628	Wolf 1061	dM4.5	10.12	12.10	−2.42	≤ 26.5	≤ −5.15	4	
643	Wolf 629	dM4	11.70	12.84	−2.71	≤ 27.0	≤ −4.43	1	
644C	VB 8	–	16.66	16.66	−4.23	26.7	−3.81	1	
687	BD+68°946	dM4	9.15	10.79	−1.90	26.9	−5.02	6	
695BC	ADS10786BC	dM3.5	10.33B	10.30B	−1.90	27.6	−4.57	2	
695BC	ADS10786BC	–	10.79C	11.29C	−2.08				
699	Bardnard's star	sdM4.5	9.54	13.25	−2.87	26.1	−5.23	2	
825	HD202560	dM1	6.67	8.75	−1.09	27.3	−5.12	6	
832	HD204961	dM1	8.67	10.33	−1.72	26.8	−5.26	6	

*Rotational velocity (V) data from Pettersen (1983).

References: 1, Johnson (1981); 2, Vaiana *et al.* (1981); 3, Cash, Charles & Johnson (1980); 4, Johnson (1983); 5, present work; 6, Golub (1983); 7, Caillault (1982); 8, Kahler *et al.* (1982); 9, Haisch & Linsky (1980).

a few hours and suggested that they are caused by changes in the active regions rather than the rotation of the star. There is perhaps a common origin for the slow variability in the X-ray and ultraviolet lines in the flare stars.

3 Discussion

3.1 Distribution of L_x/L_{Bol} for the flaring and non-flaring dwarf M stars and correlation between L_x and L_{Bol}

Besides the seven flare stars discussed in this paper, several other flaring and non-flaring dwarf M stars have been observed as part of a survey of nearby dwarf stars by Johnson (1981) and in the *Einstein* stellar survey of Vaiana *et al.* (1981). A few other individual flare stars like YZ CMi, Proxima Cen etc. have been observed by other investigators in order to study their X-ray flaring activity (Kahler *et al.* 1982; Haisch *et al.* 1983). Note that all the flare stars observed with the

Einstein were detected in X-rays. It may also be pointed out that these flare stars do not represent either an X-ray flux limited or magnitude limited sample.

In order to study the properties of all the X-ray detected flare stars and other dwarf M stars from the viewpoint of searching for a correlation between their optical, ultraviolet and X-ray emission parameters, we have made a compilation of their X-ray and optical characteristics in Table 3. The spectral type of the stars, their visual magnitude m_v, the parallax values and M_v were taken from Gliese (1969). The bolometric correction BC and values of L_{Bol} were calculated in the same manner as described in Section 2.1. The sources from which values of L_x were taken are indicated in column 9 of Table 3. Whenever necessary the L_x values were recalculated using the conversion factor of 2×10^{-11} erg per IPC count.

Table 3 includes 29 dwarf M flare stars (27 dMe stars+two dM stars) of which 10 flare stars constitute five visual binaries, both members of which are flare stars (Kunkel 1975). There are also three dKe flare stars in the list. Additionally three dMe and 15 dM (two in a visual binary) stars, which are not known to be flare stars and which were observed in the various surveys cited above, are also included in Table 3. Of these three dMe and nine dM stars were detected in X-rays and for the rest upper limits have been given. Since individual members of the binaries were not resolved in X-ray observations, the observed L_x values represent total emission from the star

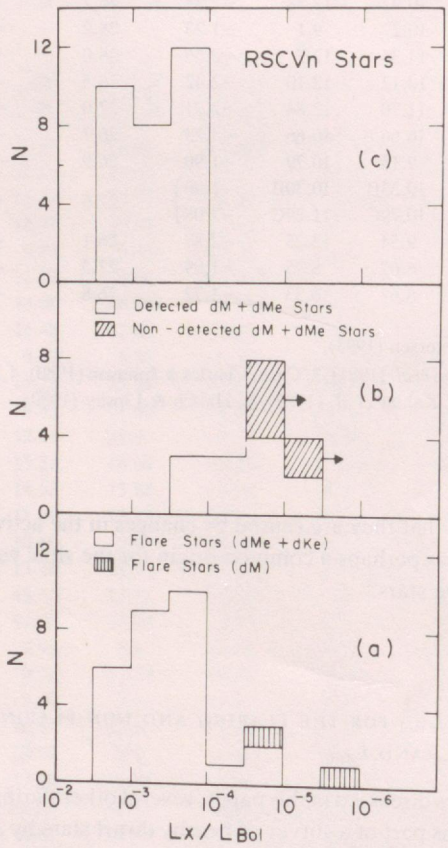

Figure 4. Distribution of the ratio of the X-ray luminosity to the bolometric luminosity (L_x/L_{Bol}) (a) for the flare stars, (b) for the non-flaring dM and dMe stars and (c) for the regular period RS CVn binaries. Arrows in (b) indicate upper limits for non-detected dM and dMe stars.

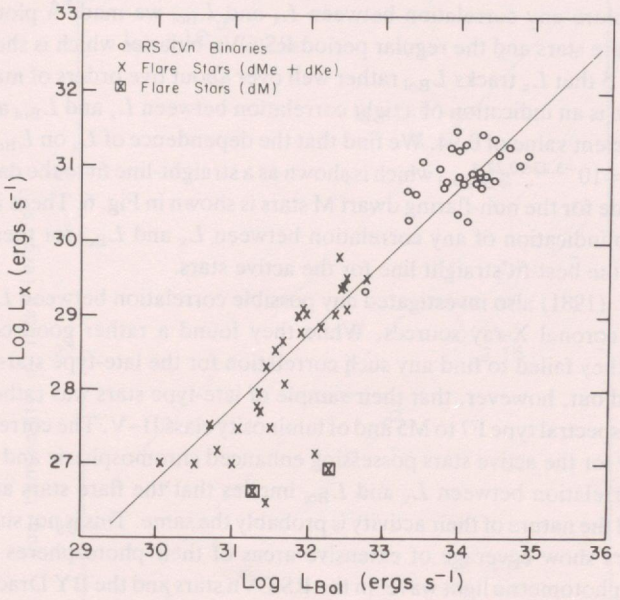

Figure 5. Plot of X-ray luminosity L_x versus bolometric luminosity L_{Bol} for the flare stars and the regular period RS CVn binaries. The straight line corresponds to the best-fit relation $L_x = 10^{-3.23\pm0.22} L_{Bol}$.

pairs. Therefore, in calculating the L_x/L_{Bol} ratio for such binaries, we used summed L_{Bol} for both members of the binary.

To investigate the existence of any systematic differences in the distribution of the ratio L_x/L_{Bol} between the flare stars and the non-flaring dwarf M stars, we made plots of the L_x/L_{Bol} distribution for these two categories of stars. These are shown in Fig. 4(a) and (b). To compare the distribution of L_x/L_{Bol} for the flare stars with that for the RS CVn binaries, which also exhibit very high chromospheric, transition region and coronal activities, we show the L_x/L_{Bol} distribution for the 30 regular period RS CVn binaries in Fig. 4(c). Values of L_x/L_{Bol} for the RS CVn stars were taken from Walter & Bowyer (1981). It will be noticed from Fig. 4 that the L_x/L_{Bol} distribution for the flare stars is markedly different from that for the non-flaring dwarf M stars but strikingly similar to that for the RS CVn binaries. A Mann–Whitney U test (Siegel 1956) was carried out to determine the probability that the distribution of L_x/L_{Bol} is similar for the flare stars and the RS CVn binaries. The computed value of the probability is 0.04 which is higher than the significance level of 0.01 usually used for large samples (in our case about 30 in each population of stars) and clearly demonstrate that both the star groups have similar L_x/L_{Bol} distributions. However, the corresponding value of the probability for the flare stars and the non-flaring dM and dMe stars is found to be 0.00003 which implies that these two populations of stars are quite dissimilar in their L_x/L_{Bol} distributions.

Notice that the two flare stars of spectral type dM have a value of L_x/L_{Bol} two to three orders of magnitude lower than that for the other flare stars. Their L_x/L_{Bol} value is comparable, however, with that of the non-flaring dwarf M stars. The mean value of L_x/L_{Bol} for the flare stars is 6×10^{-4} which agrees with the computed mean L_x/L_{Bol} value of 10.8×10^{-4} for the regular period RS CVn binaries to within a factor of 2. However, the mean L_x/L_{Bol} for the 12 X-ray-detected dM and dMe non-flaring stars is 9.6×10^{-5}, and if we also include the upper limits then it further reduces to $\leq7\times10^{-6}$. The average L_x/L_{Bol} for the non-flaring dwarf M stars is thus an order of magnitude lower than that for the flaring stars.

In order to explore any correlation between L_x and L_{Bol} we made a plot of $\log L_x$ versus $\log L_{Bol}$ for the flare stars and the regular period RS CVn binaries which is shown in Fig. 5. It is obvious from Fig. 5 that L_x tracks L_{Bol} rather well over about five orders of magnitude for these active stars. There is an indication of a tight correlation between L_x and L_{Bol} as indicated by the correlation coefficient value of 0.94. We find that the dependence of L_x on L_{Bol} is well described by the relation $L_x = 10^{-3.23 \pm 0.22} L_{Bol}$ which is shown as a straight-line fit to the data points in Fig. 5. A similar plot made for the non-flaring dwarf M stars is shown in Fig. 6. There is a large scatter of the points and no indication of any correlation between L_x and L_{Bol} for these stars. The data points fall below the best-fit straight line for the active stars.

Pallavicini *et al.* (1981) also investigated any possible correlation between L_x and L_{Bol} for the various types of coronal X-ray sources. While they found a rather good correlation for the early-type stars, they failed to find any such correlation for the late-type stars (F7 and later). It should be pointed out, however, that their sample of late-type stars was rather heterogeneous, including stars of spectral type F7 to M5 and of luminosity class II–V. The correlation that we find is applicable only for the active stars possessing enhanced chromospheric and coronal activities. The observed correlation between L_x and L_{Bol} implies that the flare stars are as active as the RS CVn stars and the nature of their activity is probably the same. This is not surprising since both categories of stars show coverage of extensive areas of their photospheres with star spots as indicated by the 'photometric light wave' in the RS CVn stars and the BY Draco variability in the flare stars. However, the underlying cause for the correlation between L_x and L_{Bol} and its physical significance are not clear at this time.

3.2 CORRELATION BETWEEN L_x AND LUMINOSITIES OF CHROMOSPHERIC AND TRANSITION REGION LINES

Linsky *et al.* (1982) have reported measurements of the fluxes of the chromospheric and transition region lines from several dMe stars and two dM stars. We converted these flux measurements to

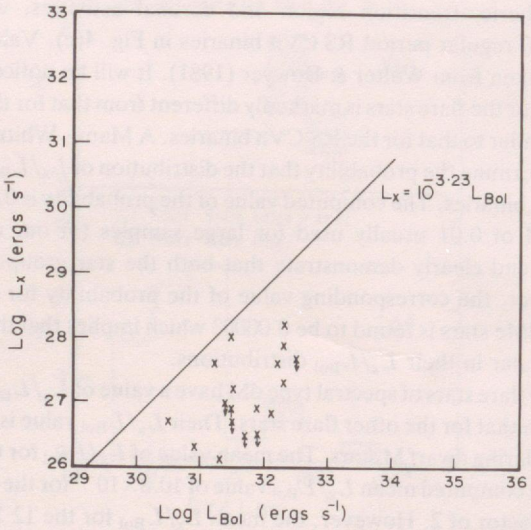

Figure 6. Scatter diagram of X-ray luminosity L_x versus bolometric luminosity L_{Bol} for the non-flaring dM and dMe stars. The straight line shows the relation between L_x and L_{Bol} for the flare stars and the regular period RS CVn binaries.

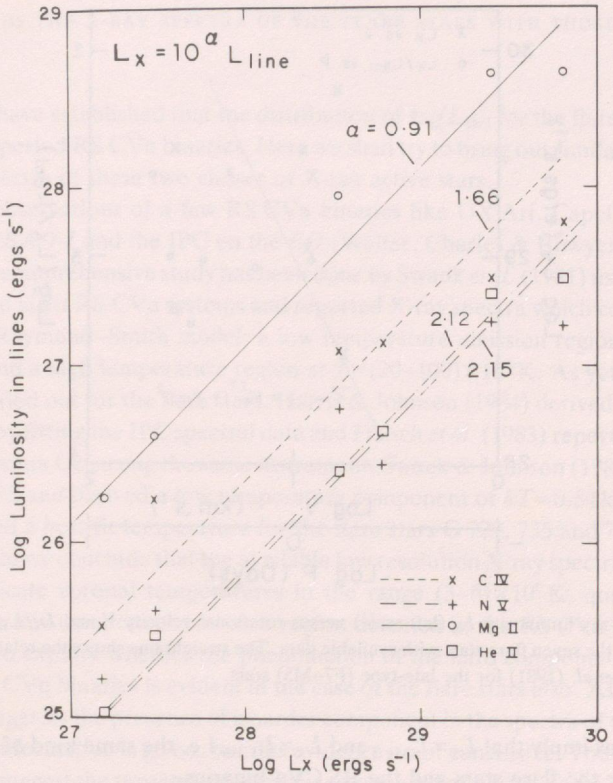

Figure 7. Plot of X-ray luminosity L_x versus luminosities in the chromospheric and transition region lines (L_{line}) for the six flare stars with available data. The continuous and broken lines correspond to the relation $L_x = 10^{\alpha} L_{line}$ where the value of α ranges between 1 and 2 for the different lines.

line luminosities for six of the stars for which L_x values are available. A plot of L_x versus the luminosities of the N v, C iv, He ii and Mg ii lines is shown in Fig. 7 for the six stars. A clear correlation between L_x and the luminosities of the individual lines is apparent from Fig. 7 for all the lines. We find that the correlation is well represented by a relation of the form $L_x = 10^{\alpha} L_{line}$ where α ranges from 1 to 2 for the different lines and its values are indicated in the figure along with the best-fit lines. The values of the correlation coefficients for the Mg ii, He ii, C iv and N v lines are found to be 0.99, 0.99, 0.97 and 0.97, respectively, which imply a rather tight correlation between L_x and the luminosities of these lines. Notice that there exists a correlation not only between L_x and the transition region line luminosities but also between L_x and L for the chromospheric Mg ii line. This suggests that in the flare stars the chromospheres, transition regions and coronae are physically related and that there is probably a common heating mechanism for them. It may be mentioned that the correlation between Mg ii emission and soft X-ray emission was also pointed out by Ayres, Marstad & Linsky (1981) for F–K dwarfs and giants. They, however, represented this correlation by a power law, e.g. $F_x/F_{Bol} \propto (F_{Mg\,II}/F_{Bol})^3$. Further they found that $F_{C\,IV}/F_{Bol} \propto (F_{Mg\,II}/F_{Bol})^{1.5}$ which taken together with the relationship between F_x and $F_{Mg\,II}$ implies that $F_x/F_{Bol} \propto (F_{C\,IV}/F_{Bol})^2$. Expressing these relations in terms of luminosities we can write $L_x L_{Bol}^2 \propto L_{MG\,II}^3$ and $L_x L_{Bol} \propto L_{C\,IV}^2$. Since $L_x \propto L_{Bol}$ for the active stars,

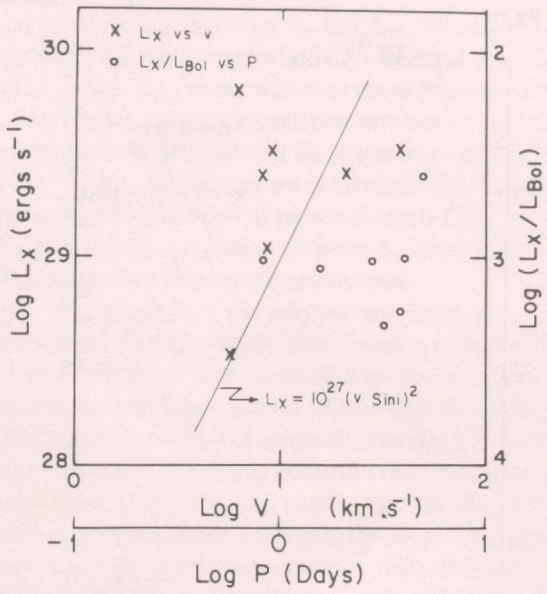

Figure 8. Plots of X-ray luminosity L_x (left scale) versus rotational velocity V and L_x/L_{Bol} (right scale) versus rotation period P for the seven flare stars with available data. The straight line shows the relation $L_x=10^{27}(V \sin i)^2$ found by Pallavicini *et al.* (1981) for the late-type (F7–M5) stars.

the above relations imply that $L_x \propto L_{Mg\,II}$ and $L_x \propto L_{C\,IV}$, i.e. the same kind of linear relationship that we found for the flare stars and the RS CVn binaries.

3.3 CORRELATION BETWEEN L_x AND ROTATION PERIOD OR ROTATION VELOCITY

Pallavicini *et al.* (1981) found a correlation between L_x and the rotation velocity ($V \sin i$) for the late-type (spectral-type F7–M5) stars which is described by the relation $L_x=10^{27}(V \sin i)^2$. For the RS CVn binaries Walter & Bowyer (1981) have claimed that $L_x/L_{Bol} \propto P^{-1.2}$ where P is the rotation period of the active star and is assumed to be the same as the binary period. We have shown previously that the L_x/L_{Bol} ratio for the flare stars is in close agreement with that for the regular period RS CVn binaries and both kinds of stars have coronae with a similar degree of activity. We therefore examined the flare star data to detect the existence of any similar correlation between L_x and P or L_x and the equatorial rotation velocity V. Unfortunately P and V data are available for only seven of the X-ray-observed flare stars. We have taken P and V values from the work of Pettersen (1983). These values are derived from photometric observations in which modulation of the star light arising from rotation of star spots present on the star's photosphere is monitored. In Fig. 8 we have plotted $\log L_x$ (left scale) versus $\log V$ and $\log L_x/L_{Bol}$ (right scale) versus $\log P$ for the seven stars. The relation of Pallavicini *et al.* (1981) is shown by a straight line in Fig. 8. We find no evidence of any correlation between L_x and V or L_x and P for the seven stars. We may mention that the validity of the relation $L_x/L_{Bol} \propto P^{-1.2}$ has been questioned by Rengarajan & Verma (1983) who point out that in the RS CVn sample of Walter & Bowyer (1981) there exists a relationship between L_{Bol} and P given by $L_{Bol} \propto P^{-1.1}$ while L_x shows no dependence on P. They therefore conclude that the relation between L_x/L_{Bol} and P results simply from the dependence of L_{Bol} on P. From our analysis of the flare stars we conclude that there is no compelling evidence for a relationship between L_x/L_{Bol} and P or L_x and V at least for the limited sample of flare stars.

3.4 COMPARISON OF THE X-RAY SPECTRA OF THE FLARE STARS WITH THOSE OF THE RS CVn BINARIES

In Section 3.1 we have established that the distribution of L_x/L_{Bol} for the flare stars is similar to that of the regular period RS CVn binaries. Here we shall try to bring out similarities between the X-ray emission spectra of these two classes of X-ray active stars.

X-ray spectral observations of a few RS CVn binaries like UX Ari, Capella etc. have been carried out with *HEAO-1* and the IPC on the *EO* (Walter, Charles & Bowyer 1978; Cash *et al.* 1978) but the most comprehensive study has been done by Swank *et al.* (1981) using the SSS on the *EO*. They observed eight RS CVn systems and reported X-ray spectra which could be fitted by a two-temperature Raymond–Smith model: a low temperature emission region in the source at $T=(4–8)\times10^6$ K and a high temperature region at $T=(20–100)\times10^6$ K. As yet no such detailed study has been carried out for the flare stars. Harris & Johnson (1984) derived a temperature of 0.3 keV for G 669 by fitting the IPC spectral data and Haisch *et al.* (1983) reported a temperature of 4×10^6 K for Proxima Cen using the same instrument. Swank & Johnson (1982) observed Wolf 630AB with the SSS and derived a low temperature component of $kT=0.54$ keV. As discussed earlier, we obtained a best-fit temperature for the flare stars G 729, 735 and 791.2 in the range $(3–4)\times10^6$ K. Hence we conclude that the available low resolution X-ray spectral observations of the flare stars indicate coronal temperatures in the range $(3–6)\times10^6$ K, quite similar to the temperature of the low component emission region detected in the RS CVn binaries.

It is interesting to explore whether the phenomenon of the hard component emission region detected in the RS CVn binaries is evident in the case of the flare stars also. As discussed earlier the present work suggests the presence of a harder component in the spectra of the two flare stars for which spectral information is given, but this evidence is not conclusive. The SSS observations of Wolf 630AB do suggest the presence of a harder component of $kT\geqslant0.7$ keV. More compelling evidence for the presence of a harder component in the spectra of the flare stars has been obtained with the *HEAO-1*. Tsikoudi (1982) searched 70 known flare stars for X-ray emission above 2 keV using the medium energy detector (MED) on board *HEAO-1*. Positive detections were reported from 10 of the flare stars. It should be noted that the error boxes derived by MED contained other objects apart from the flare stars and hence individual identifications may be suspect, but the positive results obtained from 19 per cent of the searched stars is statistically highly significant. Eight of these 10 stars for which X-ray emission is detected by the MED have also been observed with the IPC (see Table 3). We have calculated the hardness ratio defined as the ratio of the 2–10 keV X-ray flux (MED observations) to the 0.1–4 keV X-ray flux (IPC observations) for these eight flare stars. The stars G 229 and PZ Mon have unreasonably high values for the hardness ratio (72 and 35 respectively) and we suggest that identification of these objects with the X-ray sources may be coincidental. In fact the error box for G 229 contains three spiral galaxies and that of PZ Mon contains several 13–15 mag variable stars in the constellation of Monoceros. For the remaining six flare stars the hardness ratio is in the range 0.3–10.0. If the X-ray flux observed above 2 keV is the high energy tail of the 8×10^6 K plasma, the hardness ratio should be $\leqslant0.2$ (Haisch & Simon 1982). Therefore detection of hard X-rays from the flare stars is suggestive of a hard component in their spectra with a plasma temperature greater than 10^7 K, quite similar to the harder component seen in the RS CVn binaries.

All the six flare stars detected by MED for which the hardness ratio is between 0.3 and 10.0 are members of binary systems and four of them are spectroscopic binaries. This should be compared with the 50 per cent binary incidence and 20 per cent spectroscopic binary incidence among the whole sample of flare stars. It should be noted that the regular period RS CVn systems are close binaries with the binary separation being a few times the stellar radii, and the L_x/L_{Bol} distribution of the regular period RS CVn binaries is different from that of the long period binaries, whereas

the flaring and L_x/L_{Bol} behaviour of the flare stars in close binaries and of single flare stars are indistinguishable. More detailed observations with better spectral resolution are required to investigate the two-component emission behaviour of the flare stars and also to distinguish the behaviour of the binary and single flare stars.

4 Conclusions

(1) Seven flare stars were observed with the IPC on the *EO* and all were detected as X-ray sources with a mean L_x value of 2×10^{28} erg s^{-1}. The dM flare star G 229, which exhibits the weakest flaring activity, is found to have the lowest L_x value of 8×10^{26} erg s^{-1}. Except for G 229, the L_x/L_{Bol} values for the six stars lie within a factor of 4 with a mean of 4.6×10^{-4}.

(2) Analysis of the IPC pulse height data for three of the stars, namely G 729, 735 and 791.2, yields a value of $\sim3\times10^6$ K for the corona temperature for these stars.

(3) A weak X-ray flare which lasted for $\simeq$400 s with a peak value of $L_x=5\times10^{27}$ erg s^{-1} was detected in G 729. The total energy released in the 0.1–4 keV band in this flare was $\sim10^{30}$ erg. Gradual intensity variations by a factor of 1.8 over a period of about 5 hr were detected in G 735.

(4) A study of the distribution of L_x/L_{Bol} for all the X-ray-observed flare stars and non-flaring dM stars shows that the distribution of L_x/L_{Bol} for the flare stars is remarkably similar to that of the regular period RS CVn binaries, but quite dissimilar to that of the non-flaring dM and dMe stars. The mean value of the ratio L_x/L_{Bol} for the flare stars is found to be 6×10^{-4} which is comparable with the value of 10.8×10^{-4} for the regular period RS CVn binaries but is an order of magnitude higher than the value of $\leq7\times10^{-6}$ deduced for the non-flaring dM and dMe stars.

(5) A strong correlation is found between L_x and L_{Bol} for the flare stars and the regular period RS CVn binaries described by the relation $L_x=10^{-3.23\pm0.22}L_{Bol}$. The physical significance of this is not clear at present, however.

(6) A correlation is also detected between L_x and the luminosities of chromospheric and transition region lines for the flare stars. The correlation is well represented by the relation $L_x=10^{\alpha}L_{line}$ where the value of α lies between 1 and 2 for the different lines.

(7) No correlation is detected between L_x and the equatorial rotation velocity V or between L_x/L_{Bol} and the rotation period P for a limited sample of flare stars with available data.

(8) Similarities are found in the X-ray spectra of the flare stars and the RS Cvn binaries. There is a suggestion of the existence of a hard component of $T>10^7$ K in the flare star spectra similar to that observed in several RS CVn binaries.

Acknowledgments

We thank Dr F. Seward for advice and discussion on the analysis of the IPC data. We also wish to thank an anonymous referee for his comments which helped to improve this manuscript.

References

Agrawal, P. C., Rao, A. R. & Sreekantan, B. V., 1983. *Activity in Red-Dwarf Stars, IAU Colloq. No. 71*, p. 125, eds Byrne, P. B. & Rodono, M., Reidel, Dordrecht, Holland.
Ayres, T. R., Marstad, N. C. & Linsky, J. L., 1981. *Astrophys. J.*, **247**, 545.
Caillault, J. P., 1982. *Astr. J.*, **87**, 558.
Cash, W., Bowyer, S., Charles, P., Lampton, M., Garmire, G. & Riegler, G., 1978. *Astrophys. J.*, **223**, L27.
Cash, W., Charles, P. & Johnson, H. M., 1980. *Astrophys. J.*, **239**, L23.
Cristaldi, S. & Rodono, M., 1973. *Inf. Bull. Variable Stars, No. 835.*
Feix, G., 1974. *Inf. Bull. Variable Stars, No. 943.*
Gliese, W., 1969. *Catalogue of Nearby Stars, No. 22*, Veroff. Astr. Rechen-Inst. Heidelberg.

Golub, L., 1983. *Activity in Red-Dwarf Stars, IAU Colloq. No. 71,* p. 83, eds Byrne, P. B. & Rodono, M., Reidel, Dordrecht, Holland.

Gurzadyan, G. A., 1980. *Flare Stars,* p. 3, Pergamon Press, Oxford.

Haisch, B. M. & Linsky, J. L., 1980. *Astrophys. J.,* **236,** L33.

Haisch, B. M. & Simon, T., 1982. *Astrophys. J.,* **263,** 252.

Haisch, B. M., Linsky, J. L., Bornmann, P. L., Stencel, R. E., Antiochos, S. K., Golub, L. & Vaiana, G. S., 1983. *Astrophys. J.,* **267,** 280.

Harris, D. E. & Johnson, H. M., 1984. Preprint.

Heise, J., Brinkman, A. C., Schrijver, J., Mewe, R., Groenschild, E., den Boggende, A. & Grindlay, J., 1975. *Astrophys. J.,* **202,** L73.

Jarret, A. H. & Grabner, G., 1974. *Inf. Bull. Variable Stars, No. 968.*

Johnson, H. M., 1981. *Astrophys. J.,* **243,** 234.

Johnson, H. M., 1983. *Astrophys. J.,* **273,** 702.

Kahler, S., *et al.*, 1982. *Astrophys. J.,* **252,** 239.

Kahn, S. M., Linsky, J. L., Mason, K. O., Haisch, B. M., Bowyer, C. S., White, N. E. & Pravdo, S. H., 1979. *Astrophys. J.,* **234,** L107.

Kunkel, W. E., 1973. *Astrophys. J. Suppl.,* **25,** 1.

Kunkel, W. E., 1975. *Variable Stars and Stellar Evolution, IAU Symp. No. 67,* p. 67, eds Sherwood, V. E. & Plaut, L., Reidel, Dordrecht, Holland.

Lang, K. R., 1980. *Astrophysical Formulae,* 2nd edn, Springer-Verlag.

Linsky, J. L., Bornmann, P. L., Carpenter, K. G., Wing, R. F., Giampapa, M. S., Worden, S. P. & Hege, E. K., 1982. *Astrophys. J.,* **260,** 670.

Pallavicini, R., Golub, L., Rosner, R., Vaiana, G. S., Ayres, T. & Linsky, J. L., 1981. *Astrophys. J.,* **248,** 279.

Pettersen, B. R., 1980. *Astr. Astrophys.,* **82,** 53.

Pettersen, B. R., 1983. *Activity in Red-Dwarf Stars, IAU Colloq. No. 71,* p.17, eds Byrne, P. B. & Rodono, M., Reidel, Dordrecht, Holland.

Raymond, J. C. & Smith, B. W., 1977. *Astrophys. J. Suppl.,* **35,** 419.

Rengarajan, T. N. & Verma, R. P., 1983. *Mon. Not. R. astr. Soc.,* **203,** 1035.

Siegel, S., 1956. *Non-parametric Statistics for the Behavioural Science,* McGraw-Hill, Kogakusha Ltd.

Swank, J. H. & Johnson, H. M., 1982. *Astrophys. J.,* **259,** L67.

Swank, J. H., White, N. E., Holt, S. S. & Becker, R. A., 1981. *Astrophys. J.,* **246,** 208.

Tsikoudi, V., 1982. *Astrophys. J.,* **262,** 263.

Vaiana, G. S. *et al.*, 1981. *Astrophys. J.,* **245,** 163.

Walter, F. M. & Bowyer, S., 1981. *Astrophys. J.,* **245,** 671.

Walter, F. M., Charles, P. & Bowyer, S., 1978. *Astrophys. J.,* **225,** L119.

PROCEEDINGS OF INTERNATINAL SYMPOSIUM ON COSMIC RAY SUPERHIGH ENERGY INTERACTIONS

Oct. 29 - Nov. 3 1986

国際宇宙線超高能作用討論会

中 国 北 京

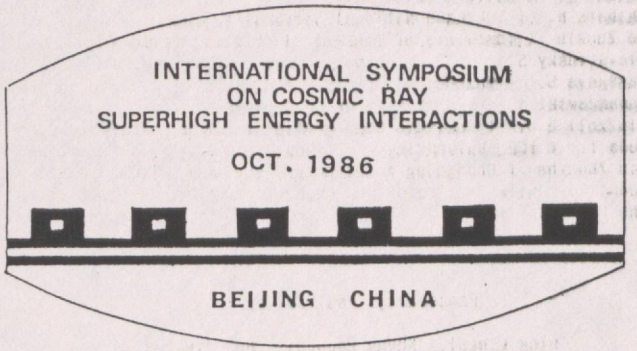

INSTITUTE OF HIGH ENERGY PHYSICS, ACADEMIA SINICA
SHANDONG UNIVERSITY
YUNNAN UNIVERSITY
ZHENZHOU UNIVERSITY
CHONGQING ARCHITECTURE ENGINEERING COLLEGE

A Study of the Composition of Primay Cosmic Rays at High Energy

V.K.Balasubrahmanyan
NASA/Goddard Space Flight Center
Code 661, Greenbelt, Maryland, 20771, USA

B.V.Sreekantan
Tata Institute of Fundamental Research
Homi Bhabha Rd., Colaba, Bomaby, 400005, India

J.A.Goodman and G.B.Yodh
Department of Physics and Astronomy
University of Maryland, College Park, Md., 20742, USA

Abstract

Direct measurements of energy spectra of primary cosmic rays are compared with indirect determination of the all particle energy spectrum from study of air showers and other measurements to infer changes in the elemental mix near the "bend" at about 10^{15}eV. We find that there is no evidence for the dominance of protons or the presence of a new proton component at 10^{15} eV . There is some evidence that cosmic ray spectra of elements with Z>2 may be harder above 5×10^{14} eV than at lower energies. A possible new balloon experiment to determine the flux of silicon and iron group nuclei at energies greater than 10^{13} eV with well defined acceptance and charge determining capability is discussed.

I. Introduction

Properties of primary cosmic rays in the energy region 10^{11} to 10^{16} eV are of considerable importance for testing different models of origin, propagation and acceleration of cosmic rays. Current popular models involving shock acceleration mechanisms predict a universal spectral slope and a rigidity dependent steepening above 10^{14} eV (Cesarsky and Lagage 1981, Axford 1981). One expects a change in the mix of primary elemental species above such energies. The average mass of cosmic rays is expected to change in the two decades near the observed 'bend' at $\sim 10^{15}$ eV. In this paper we make a careful study of the available data and attempt to determine the implied changes in the composition . Several 'direct' and 'indirect' experiments provide the data for this study.

By direct experiments we mean those in which individual primaries are recorded, their charge and energy determined using instruments with well defined aperture flown at balloon or satellite altitudes. In these experiments, in addition to identifying the incident primary particle and determining its energy, the corrections for the loss or gain of particles due to collisions with air nuclei are reasonably well determined (Grigorov et al 1971, Ryan et al 1972, Juliusson 1974, Simon et al 1980, Mandritskaya et al 1985 and Burnett et al 1983 and 1985).

Indirect experiments are those where the energy and the nature of the incoming particle can only be inferred by detailed simulations of the observations of cascade progeny. The mass resolution of these experiments is poor and only general trends can be extracted from the analysis of these indirect air shower measurements (Khristiansen et al 1983, Efimov et al 1983, La Pointe et al 1968, Bradt et al 1965, Hara et al 1981, Acharya et al 1983).

II. The All Particle Spectrum

The integral spectrum from direct measurements of Grigorov et al (1971) and Burnett et al (1983 and 1985) along with the experimental points of Khristiansen et al (1983) derived from extensive air shower size spectrum measurements made with the Moscow State University array at sea level, are shown in figure 1. The figure does not include the points based on the analysis of cascade profile development in the atmosphere (Bradt et al 1965) and those derived from Cerenkov density spectrum measurements (Efimov et al 1983). We shall discuss later our reasons for not including these data. The size spectra of other groups, Hara et al (1981) and Acharya et al (1983) , essentially agree with those of Moscow State University, hence

the energy spectra derived from them are not plotted in the figure.

It is clear from figure 1 that there is good agreement between the results of Grigorov et al (1971) and Burnett et al (1983 and 1985) in the overlapping regions. The all particle spectrum over the entire energy range, 10^{11}-10^{15} eV, can be well represented by a single power law (the full line in figure 1) corresponding to an exponent (-1.63 ± .02) (Gaisser and Yodh 1980). It can also be seen from figure 1 that air shower results agree with the all particle spectrum from direct measurements in the overlapping region. While there is clear indication of a steepening of the all particle spectrum around a few times 10^{15} eV, there is no evidence for any other features - either a flattening of the spectrum at 10^{14} eV or a hump just before the steepening. These features seem to creep into the spectral distribution when they are plotted by multiplying the intensities by factors like $E^{1.5}$ to cover a wide energy range in a single plot and to magnify departures from a single power law. Since the original data is generally not available in tabular form, it becomes necessary to read both the intensity values and the corresponding energy values from the published log-log plots. To illustrate the type and magnitude of errors that arise by this procedure, we have plotted in figure 2 the data of figure 1 as read by two different observers, multiplying the intensity values by the factor $E^{1.5}$. We also show in the figure the best fit line to the spectrum given in figure 1, suitably transformed. We have not plotted points from the JACEE all particle spectrum from figure 1, in figure 2 because the JACEE experiment papers do not specify the energy uncertainties in their individual data points and therefore it is impossible to correctly assign significance to the scatter that will be introduced in firgure 2 if these points were included.

It is seen that the same data points which were close to the best fit line in figure 1 now show a considerable scatter. The point to be emphasised is that these deviations are not due to the statistical errors in the original data, which were really small, but rather due to errors that have been introduced in reading the intensity and energy values from the integral plots. It is difficult to estimate the magnitude of these reading errors. The deviations become even more pronounced if plots of differential spectra are made from graphs of integral spectra, and can often lead to misleading judgements.

The apparent enhancement in the primary flux around a few times 10^6 GeV discussed by various authors (Wdowczyk and Wolfendale (1983), Fichtel and Linsley (1986)) is based upon interpretation of graphs of differential primary spectra multiplied by $E^{2.5}$ (or integral spectra multiplied by $E^{1.5}$)

which are derived from air shower observations and compared with those from direct measurements. We feel that these plots do not correctly display the errors or spread of the points derived from air shower data and that the errors are grossly underestimated or ignored. This point is easily argued by the following discussion. Air shower experiments in the energy range extending from 10^5 GeV to 10^7 GeV measure either shower size or Cerenkov photons. The observed quantity has to be converted to primary energy using simulations. Typical fluctuations of shower size from primaries of fixed energy are large. For instance, for showers generated by proton primaries of 500 TeV the fluctations in the mean shower size even at shower maximum are $\sim$ 18 percent and at greater depths beyond the maximum are as large as 50 percent (Wrotniak and Yodh 1985). Let us assume that shower size to energy conversion has f percent fluctuations. In deriving the primary energy spectrum the statistical errors on the number of events must be convoluted with these fluctuations. Roughly speaking, this will introduce a spread in the primary intensity of f multiplied by the value of the slope of the primary spectrum. The primary energy estimate will also have an f percent spread. This is again magnified when one takes $E^{2.5}$ times the flux. For a f of 20 percent, a particular point on the $E^{2.5}$ dJ/dE graph should have an intensity spread of 2.5 to 0.25 times the nominal value calculated at the mean energy value. In addition, there exist sytematic diferences between results of simulations used by different experimenters which may be larger than this. One must also note that the spread due to the fact that the primary composition is mixed has to be considered. One must conclude, therefore, that the presence or the absence of a hump cannot be substantiated by the data. The only fact that is free of this problem to a great extent is the change of slope of the all particle spectrum beyond 10^7 GeV - the presence of a bend.

III. Air Shower Methods; A Critical Examination

All methods of obtaining the spectrum and composition from extensive air showers are indirect. Among these the method based on measurement of size spectrum (of electrons, muons or Cerenkov radiation) is perhaps the most reliable one. In this technique the lateral density distribution of one or more of these components is measured in individual showers by an array of large area detectors at the observation level. Integrating the lateral distribution over the shower plane, the total number of electrons, muons or Cerenkov photons is determined and the total energy of the primary particle is estimated with the aid of detailed Monte Carlo simulations. The simulations show that even under varying assumptions for interaction characteristics, a given observed shower size can be related to the primary

energy within a factor of $\sim$ 2, provided the difference in the steepness of the lateral distribution for different primary nuclei is taken into account.

A second method used by the Chacaltaya (Bradt et al 1965),Akeno (Hara et al 1981) and Tien Shan (Danilova et al 1977) groups is to relate the estimated shower size at shower maximum to the primary energy. If the shower maximum and the corresponding size are determined in individual showers as in the case of the Fly's Eye experiment (Baltrusaitis et al 1984), this would indeed be a reliable method. The threshold for the Fly's Eye experiment at present is rather high, $\sim 10^{17}$ eV. At smaller sizes one uses the "constant intensity cut method ", in which sizes of different showers giving the same counting rate at different zenith angles are first determined and then from a plot of shower size versus the slant atmospheric depth, the height of shower maximum in the vertical direction and the corresponding shower size is deduced. The shower size at maximum is then related to the primary energy. The existing discrepancies and uncertainties involved in this method have been discussed in detail by Linsley (Linsley 1983). Furthermore, it should be noted, the measured parameters of an individual shower cannot be related to the primary energy, in contrast to the size spectrum method. In addition, the fluctuations in the location of shower maximum and size at maximum for different atomic species of the same total energy are different, this leads to underestimation of the errors in conversion of size at maximum to energy.

An even more indirect method - the Cerenkov density spectrum method - has been use by Efimov et al (1983). In this experiment the Cerenkov density spectrum is measured for photon density range from 17 to 1480 photons/cm^2. A measured Cerenkov density spectrum at the observational level does not correspond to a particular primary energy. What has been done by Efimov et al (1983) is to establish through simulations a correspondence between a measured Cerenkov density interval and a primary energy interval. They assumed power law spectra with varying exponents and cut off energies to optimize the agreement with the observed density spectrum. The general trend of primary spectra can be established from such experiments. Reliance, however, should not be placed on the very small errors shown for individual data points. The intensity for primary all particle flux given by Efimov et al (1983) agrees very well with the value measured by Grigorov et al (1971). It is, however, not clear from the paper of Efimov et al(1983) whether they normalized the intensity with that of Grigorov et al(1971). Even if one does not attach special significance to the individual data points of Efimov et al (1983) it is clear that their results on the change of spectral index should be taken seriously; the primary integral spectrum

being a power law with an exponent (-1.63±.03) at energies below 2×10^{15} eV, steepening to an exponent of (-2.3±.04) at energies greater than 5×10^{15} eV.

We now make a general comment regarding deriving the all particle spectrum from air shower measurements. For clarity of discussion let us assume that the primary cosmic ray beam has only one species, say protons. Let us discuss experiments which measure number spectra or Cerenkov photon spectra. Number spectra show a bend at some shower size N_1 which depends on altitude (see Hillas 1984 and Khristiansen et al 1980). For $N < N_1$ number spectrum is described by the power law $N^{-2.5}$, steepening to $N^{-3.1}$ for $N > N_1$. The relationship between shower size and the average primary energy responsible for these showers may be approximated by $E_0 = B \times N^{\alpha}$ where $\alpha > 1$ for experiments done at depths beyond the shower maximum (see for example J.F.de Beer et al 1968). The spectral index for the number spectrum that would result from a primary spectrum $dJ/dE \sim E^{-\gamma}$ can be shown to be $N^{-\beta}$ where $\beta = (\gamma+\alpha-1)/\alpha$. Typically, one finds that for a primary spectral index $\gamma = 2.7$ one gets $\beta = 2.48$ and for $\gamma = 2.5$ one gets $\beta = 2.3$,respectively, if $\alpha = 1.15$. The observed slope of the number spectrum of $\beta > 2.5$ would rule out a primary spectrum with a slope of 2.5. To illustrate this quantitatively, we have simulated the number spectrum at seal level using a large sample of Monte Carlo showers using a particular non-scaling model which fits ISR and SPS pbarp data (the model M-F00 of Wrotniak and Yodh 1985) for two different compositions ; a proton dominant model proposed by Linsley at Bangalore (Linsley 1983) and a common rigidity cut off model proposed by the Maryland group (Mincer et al 1985). The results are shown in figure 3 where data are compared with simulations. Difficulties with the proton dominant model are clearly seen. The conclusion is that one cannot have a very flat spectral index for protons between 10^5 to 10^7 GeV.

IV. Measurements of Individual Components

(a) Protons:

We have shown in figure 1 direct measurements of the proton and alpha spectra (Simon et al 1980, Ryan et al 1972 and Burnett et al 1983 and 1985). The JACEE experiment (Burnett et al 1983 and 1985) shows no abrupt change of slope for protons in the energy domain 5×10^{12} to 10^{14} eV. In this respect it disagrees with the results of Grigorov et al (1971) which indicated a steepening of the proton spectrum at 10^{12} eV and of Mandritskaya et al (1985) which shows steepening around 10^{13} eV. The

absolute fluxes of all three experiments are in essential agreement around 10^{12} eV, and agree with the extrapolation from the measurements of Ryan et al (1972).

The sea level muon spectrum deduced from intensity as a function of depth and angular distribution of penetrating particles in deep underground experiments (Klemke et al 1981) and from muon spectrograph measurements (Kitamura et al 1981) have been interpreted to rule out steepening of the proton spectrum at as low an energy as 10^{12} or 10^{13} eV.

The large emulsion chamber experiments at Chacaltaya (Lattes et al 1980), Mt. Fuji (Amenomori et al 1982,1985a,1985b;Akashi et al 1981), Pamir (Borisov et al 1985) and Kanbala (Ren et al 1985) have been analyzed to show that if the JACEE proton spectrum continues without change of slope beyond 10^{14} eV, the flux of high energy gamma ray and hadron families should have been higher by a factor of ~ 3 , even under the assumption that these family events arise only from the collisions of protons (Akashi et al 1981). This conclusion is unchanged even if one assumes strong scale violations in the fragmentation region. Recently, Gaisser and Stanev (1982) have demonstrated that these family events could arise in the collisions of heavy primaries in the atmosphere also. This would require the proton flux to be lower at energies greater than 10^{14} eV, in other words, a steepening rather than a flattening of the proton spectrum.

The necessity for steepening of the proton spectrum around 10^{14} eV is also evident from the delayed hadron experiments of the Maryland group (Goodman et al 1982). Their detailed simulations show that the trigger rate in their experiment would be higher than the observed rate by a factor greater than 3 if the proton spectrum continued without change of slope upto 10^{15} eV. The spectra of uncorrelated hadrons and gamma rays at mountain altitudes also require the same conclusion (Akashi et al 1981). A proton dominant model would also have difficulty in interpreting the data on lateral distribution of hadrons in showers of size 10^5 at sea level (Kellerman and Hillas 1981) which are generated by primaries of about 10^{15} eV.

(b) Alpha Particles:

The α-particle spectrum, shown in figure 1, can be represented by a power law with an exponent (-1.83±.2) We note that the α-particle flux is lower compared to the proton flux by a factor of four around 10^{14} eV per nucleus.

These three results : (1) the steepening of the all particle spectrum beyond a few times 10^{15} eV, (2) the steepening of the proton spectrum around 10^{14} eV, and (3) the fact that the α-particle flux is lower than the proton flux around 10^{14} eV per nucleus, point to the need for an increasing fraction of heavier nuclei (Z>2) to make up the all particle flux beyond 10^{14} eV .

(c) Nuclei with Z>2 :

The JACEE experiments have now reported flux values for the heavier components of cosmic rays beyond 10 TeV/nucleon for the carbon/oxygen (CNO) and neon/silicon (MH) species and upto 2 TeV/nucleon for elements with Z >17. In figure 5 we have plotted these latest results converting energy per nucleon into total energy (energy per nucleus) assuming mean atomic mass values of 15, 26 and 56 for the three groups respectively. In the same figure, for purposes of comparision, we have reproduced the all particle spectrum from figure 1.

It is seen from figure 5 that all the heavier components retain their power law behaviour, consistent with low energy trends reported in the measurements of Simon et al (1980) and Juliusson (1974). At energies beyond 10^{13} eV per nucleus there is a tendency for the total flux of heavier components to approach the all particle flux.

At this point, we discuss, again, indirect air shower methods used to investigate the composition of primary cosmic rays at energies where direct measurements do not exist. The variation with shower size of some of the secondary components in the shower(muons and hadrons), their fluctuations and the fluctuations in the heights of cascade maximum are other indirect methods that have been used for obtaining information on the primary composition. While these methods could be quite effective in principle, and are the only ones available at energies beyond the reach of direct experiments, it has been emphasised that these are sensitive to characteristics of high energy collisions (cross sections, multiplicities, composition of secondaries etc.) and to differences between proton-proton, proton-nucleus and nucleus- nucleus collisions.

Several studies have inferred a proton dominant or a " normal " composition at the bend from analysis of air shower data on muon and electrons and their fluctuations (Kirov et al 1980, Wolfendale and Wdowczyk 1983 and Fichtel and Linsley 1986). A detailed study of some of the data used by

these authors was also carried out by Yodh et al (Yodh et al 1984) who did full Monte Carlo simulations of the experiments to show that when showers are grouped according to fixed shower size the sensitivity of the number of muons and their fluctuations to primary composition is significantly reduced. In fact, it was found in this study that the data on muons and their fluctations for showers of a given size cannot discriminate between models which assume energy independent low energy compostion and those which have enhancement of nuclei with $Z > 4$ near 10^6 GeV due to a rigidity dependent cut off. These effects arise even in showers of well determined size, because of fluctuations in the points of interactions which in turn depend on the atomic mass of the primaries. These fluctuations when convoluted with the steep primary energy spectrum lead to the feature that protons dominate showers selected or grouped according to their size reducing the sensitivity to the primary composition unless the primaries have only one component.

It is therefore very essential that the range of direct experiments be extended to as high an energy as possible with balloon and satellite borne instruments.

V. Summary of Observations

The experimental results that have a bearing on the spectrum and compostion of primary cosmic rays in the energy range 10^{11} to 10^{16} eV may be summarised as follows :

(1) All particle spectrum is best represented by a power law in energy with an exponent (-1.63±0.02) upto 10^{15} eV. There is no indication of a flattening of the spectrum around 10^{14} eV nor of a hump around 10^{15} eV.

(2) All particle spectrum steepens around an energy of a few times 10^{15} eV.

(3) Proton spectrum in the energy range 10^{11} to 10^{14}eV is a power law with an exponent (-1.78±0.13).

(4) It is necessary that the proton spectrum steepens around a few times 10^{14} eV, at least a decade earlier than the all particle spectrum in order to account for the results on gamma families, muons, and hadrons in air showers.

(5) Alpha particle spectrum in the range upto 10^{14} eV can be repre-

sented by a power law with an exponent (-1.83±0.2). The flux of *alphas* around 10^{a4} eV is smaller than that of protons.

(6) Cosmic rays with Z>2 appear to become fractionally more important in the primary spectrum in the two decades of energy beyond the steepening of the proton spectrum around 10^{14} eV.

(7) If a second proton component (Fichtel and Linsley 1986) is invoked to explain the features of very high energy showers, it could come in and become prominant only beyond 10^{16} eV.

VI. Discussion

In the light of these findings it is clear that it is very important to extend the range of direct experiments to as high an energy as possible, especially to establish the importance of heavy components relative to the lighter ones in the energy region beyond 10^{13}eV. Of course, a long exposure of a fine grained calorimeter on space platform with an acceptance of 30 m^2sr would be one of the best ways to investigate the region around 10^{15} eV. A step in this direction has been recently taken by the Chicago group (Muller D., 1982), who flew a Cerenkov - Transition radiation detector of large area in the Space Shuttle to investigate the spectra of primary cosmic rays with $Z > 2$ upto a few TeV per amu. We await their results with great interest.

The balloon experiment of Sood and Panettievi (1981 and 1983) based on Cerenkov threshold technique was also a step in this direction. This experiment was based on a very elegant method, first proposed by Gough (1976), which uses the fact that the threshold for emission of Cerenkov radiation can be very high in the upper layers of the atmosphere due to the very low refractive index of air (for example ,the energy threshold is given by the Lorentz factor γ=3000 at 3 gm cm^2). The Z^2 dependence of Cerenkov radiation makes it feasible to detect Cerenkov light emitted by heavy nuclei like iron and discriminate comfortably against protons and low Z nuclei. In Sood's experiment two parabolic mirrors, each of area 1 m^2 , were mounted adjacent to each other with photomultipliers placed at their focii operated in coincidence. The apparatus was flown on a balloon at an altitude of 34 kms on a moonless night in December 1981. The field of view of each mirror was 7.5° corresponding to a solid angle of 0.054 steradian. The light detection level gave an estimated energy threshold for iron nuclei of 3×10^{13} eV per nucleus. At the float altitude 16 concidences were recorded in six and a half hours. Four events were identified by Sood as

possible candidates for iron nuclei. Assuming a light pool area of 1050 m^2 he estimated a geometric fator of 56.7 m^2,sr for his system. An integral flux of iron nuclei of 3×10^{-10} $cm^{-2}sr^{-1}s^{-1}$ was obtained. This flux was an order of magnitude lower than the expectations based upon linear extraploations from lower energies that we discussed in the previous sections.

On the basis of detailed Monte Carlo simulations, however, Yodh et al (1985) have found that under the conditions of Sood's experiment the effective Cerenkov light pool, which is energy dependent, is much smaller than the 1050 m^2, varying from 200 m^2 to 50 m^2 as the photon threshold is varied from 1000 photons/ m^2 to 2000 photons/m^2. The effective geometric factor for the highest pulse height events was calculated to be only 2.7 m^2,sr ; a factor 20 smaller than the factor used by Sood to calculate the flux. They also find that twelve of the sixteen events recorded by Sood could be candidates for heavy primaries and the flux observed could be much larger than that estimated by Sood.

Apart from the fact that the simulations of Yodh et al(1985) lead to a higher flux of iron nuclei than estimated by Sood, they open up the possibility of designing a more direct experiment using the same Cerenkov technique. Two major modifications to the Sood experiment are suggested. The first is to use a cylindrical plastic tube coated with wavelength shifter to detect Cerenkov photons along the mirror axis. The length of tube is such that the solid angle acceptance can be increased over that of Sood by a factor of ten. The second is to associate a double layered proportional counter assembly of reasonable dimensions for balloon payload - 30m^2- with the Cerenkov set up. With this arrrangement one can ensure that the majority of nuclei that give rise to detected Cerenkov radiation will traverse the counter assembly. This will make it possible to identify the charge of the nuclei through a measurement of their ionization loss, and also a precise definition of the effective area and geometric factor. It will also make it possible to detect lower Z primaries of high energy. Simultaneous detection of silicon and iron groups would greatly improve the quality of the experiment. Furtheremore, by using ultraviolet light sensitive detection technique the signal to noise ratio (from the background of night sky photons) can be improved. This improvement arises from the fact that the intensity of Cerenkov emission is more in the ultraviolet than in the optical while the starlight background is considerably lower in the ultraviolet than in the optical. The detection of ultraviolet light can be achieved by using wave shifter techniques. An experiment is under design based upon these considerations and will be reported elsewhere

A schematic diagram of such a modified instrument is shown in figure 5 . The combination of the increased solid angle and concidence with the proportional counter layers will increase the data collection in typical flights by at least a factor of twenty over that achieved by Sood. For the fluxes shown in figure 4 one could obtain 90 events of iron group with $E > 5 \times 10^{13}$ eV per nucleus and over 300 events of the silicon group with $E > 2.8 \times 10^{13}$ eV per nucleus in a single six hour balloon flight.

This work was supported in part by the National Science Foundation. One of us (BVS) would like to thank Dr. S. Holt, Chief of the Laboratory for High Energy Astrophysics at NASA Goddard Space Flight Center for hospitality.

References

Acharya B.S. ,et al, Proc. 18th. Int. Conf. on Cosmic Rays, Bangalore, India, **9**, 162, 1983.

Akashi , et al, Phys. Rev., **D24**, 2353, 1981.

Amenomori M., et al, Phys. Rev., **D25**, 2807, 1982.

Amenomori M., et al, Proc. 19th Int. Conf. on Cosmic Rays, La Jolla, Ca, USA, **2**, 206, 1985a.

Amenomori M., et al, Proc. 19th. Int. Conf. on Cosmic Rays, La Jolla, Ca, USA, **6**, 208, 1985b.

Axford W.I. , Proc. 17th. Int. Conf. on Cosmic Rays, Paris, France, **12**, 155, 1981.

Baltrusaitis R.M., et al, Phys. Rev. Letters, **52**, 1380, 1984.

Borisov A.S., et al, Proc. 19th. Int. Conf. on Cosmic Rays, La Jolla, Ca, USA, **6**, 200, 1985.

Burnett T.H., et al, Phys. Rev. Letters, **51**, 1010, 1983.

Burnett T.H., et al, Proc. of Int.Symp. on Cosmic Rays and Particle Physics, Ed. by A.Oshawa and T.Yuda, Inst. of. Cosmic Ray Research, Tokyo, Japan, p 468, 1985a.

Burnett T.H., et al, Proc. 19th Int. Conf. on Cosmic Rays, La Jolla, Ca, USA, **2**, 48 ,1985b.

Bradt H., et al, Proc. 9th Int. Conf. on Cosmic Rays, London, England, **2**, 715, 1965.

Cesarsky C.J. and Lagage P.O., Proc 17th. Int. Conf. on Cosmic Rays, France, Paris, **2**, 335, 1981.

Danilova T.V., et al, Proc. of 15th Int. Conf. on Cosmic Rays, Plovdiv, Bulgaria, **8**, 129, 1977.

Efimov M.N. et al, Proc. 18th Int. Conf. on Cosmic Rays, Bangalore,

India, **6**, 228, 1983.

Fichtel C. and Linsley J., Ap. J.**300**, 474, 1986

Gaisser T.K. and Yodh G.B., Ann. Rev. of Nucl. and Part. Sc., **30**, 475, 1980.

Gaisser T.K. and Stanev T., Proc. of Workshop on Cosmic Ray Int., La Paz, Bolivia, **2**, 280, 1982.

Goodman J.A., et al, Phys. Rev., **D26**, 1043, 1982.

Gough M.P., J. of Physics, **2**, 965, 1976.

Grigorov N.L.,et al, Proc. of 12th Int. Conf. on Cosmic Rays, Hobart, Tasmania, **2**, 206, 1971.

Hara T., et al, Proc. 17th Int. Conf. on Cosmic Rays, Paris, France, **11**, 250, 1981.

Hillas A.M., Proc. of 4th Moriond Astrophysics Conf.,1984.

Juliusson E., Astrophysical Journal, **191**, 331, 1974.

Kellerman E. W. and Hillas A. M. ,Proc. of 17th Int. Conf. on Cosmic Rays, Paris, France, **6**, 223 and **11**, 436, 1981.

Khristiansen G.B., Kulikov G. and Fomin J., Cosmic Rays of Superhigh Energies.Verlag Karl Themig, Munich, p 147,,1980.

Khristiansen G.B..et al, Proc. 18th Int. Conf. on Cosmic Rays, Bangalore, India, **9**, 195, 1983.

Kirov I.N. et al, Proc. of the Int. Seminar on Cosmic Ray Cascades, Sofia, Bulgaria, p. **61**, 1980.

Kitamura M.K. et al, Proc. 19th Int. Conf. on Cosmic Rays, La Jolla, Ca, USA, **9**, 159, 1985.

Klemke G., et al, Proc. of 17th Int. Conf. on Cosmic Rays, Paris, France, **9**, 151, 1981.

La Pointe M., et al, Can. J. of Phys., **46**, 565, 1968.

Lattes C.M.G., et al, Phys. Rep., **165**, 152, 1980.

Linsley J., Proc. 18th Int. Conf. on Cosmic Rays, Bangalore, India, **12**, 135, 1983.

Mandritskaya K.V., et al, Proc. 19th. Int. Conf. on Cosmic Rays, La Jolla, Ca, USA, **6**, 228, 1985.

Mincer A.I., et al , Proc. 19th Int. Conf. on Cosmic Rays, Lajolla, Ca, USA, **2**, 201, 1985.

Ren J.R., et al, Proc. 19th Int. Conf. on Cosmic Rays, La Jolla, Ca, USA, **6**, 439, 1985.

Ryan M., et al, Phys. Rev. Letters, **28**, 985, 1972.

Simon M., et al, Astrophysical Journal, **239**, 712, 1980.

Sood R.K. and Panettievi J., Nucl. Inst. and Methods, **185**, 427, 1981.

Sood R.K., Nature, **301**, 44, 1983.

Wdowczyk J. and Wolfendale A.W., Nature, **306**, 347, 1983. See also Wolfendale A.W., Reports on Prog. in Physics, **47**, 655, 1984.

Wrotniak J.A. and Yodh G.B., Proc of 19th Int. Conf. on Cosmic Rays, Lajolla, Ca., USA, **6**, 56 and **7**, 1, 1985.

Yodh G.B., Goodman J. A.. Tonwar S. C. and Ellsworth R. W. , Phys. Rev., **D29**. 892, 1984.

Yodh G.B. and Goodman J.A., private communication 1985.

Figure Captions

Figure 1. The integral all particle spectrum obtained from the observations of Grigorov et al (1971) and Burnett et al (1983) as well as the air shower results of Khristiansen et al (1983) are shown. The spectrum is well described by a single power law upto about 10^{15} eV after which the spectrum steepens. Also shown for comparision are the integral energy spectra for protons and helium nuclei.

Figure 2. This figure displays the spectra shown in figure 1 transformed by multiplying the integral intensity by $E^{1.5}$. This procedure is usual in the EAS studies to represent data over a wide range of energies so as to emphasize their deviations from a single power law. However, as discussed in the text errors creep into these plots when they are constructed by trying to read miniscule log-log plots. The JACEE data points have not been plotted for reasons described in the text.

Figure3: This figure compares the number spectrum measured at sea level with that predicted for a proton dominant primary composition (Linsley 1983), and for a spectrum used by the Maryland group (Mincer et al 1985). The differential number spectrum multiplied by $N^{2.5}$ is shown. The figure shows that a flat proton spectrum leads to disagreement with the observation.

Figure 4. A compilation of the energy spectra of different nuclear groups in primary cosmic rays compared with the all particle spectrum. Note the tendency for the flux of heavier nuclei to approach the all particle spectrum beyond 10^{13} eV.

Figure 5. A schematic diagram of the proposed detector for studying the flux of primary cosmic rays of high energy (Lorentz factor greater than 1000) with Z greater than 12.

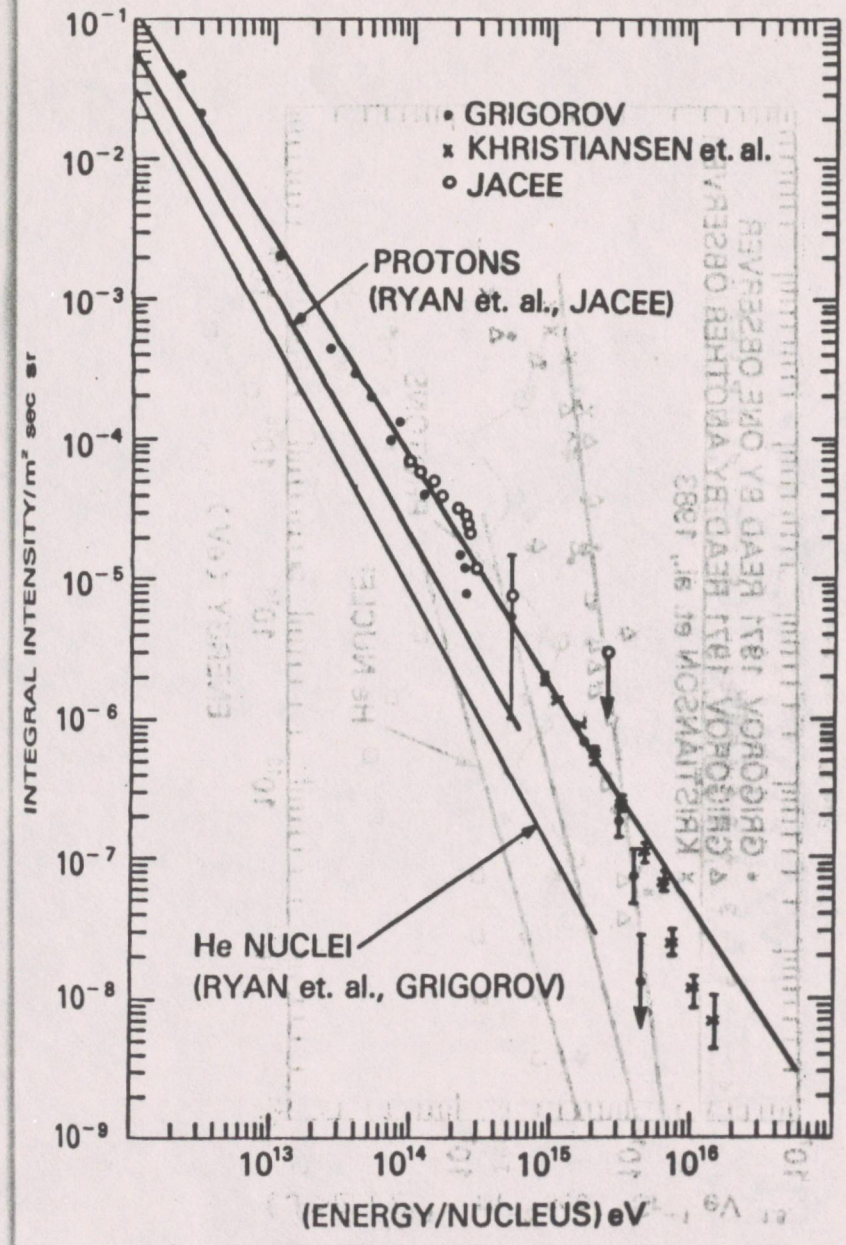

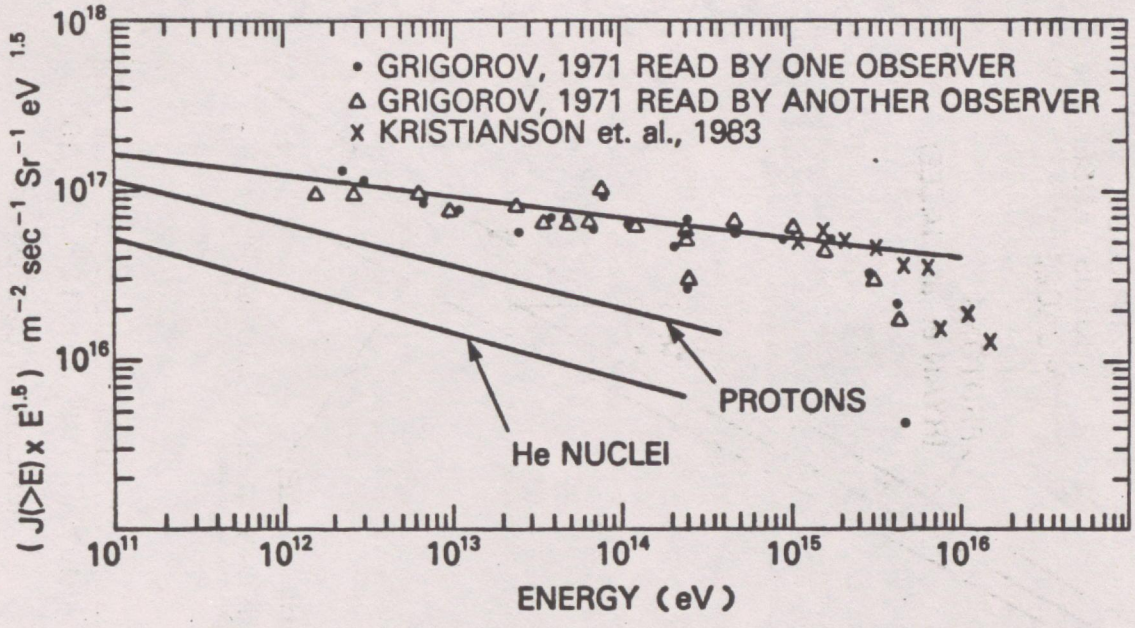
• GRIGOROV, 1971 READ BY ONE OBSERVER
△ GRIGOROV, 1971 READ BY ANOTHER OBSERVER
x KRISTIANSON et. al., 1983
PROTONS
He NUCLEI
(J(>E) x E^1.5) m^-2 sec^-1 Sr^-1 eV^1.5
ENERGY (eV)

81-9

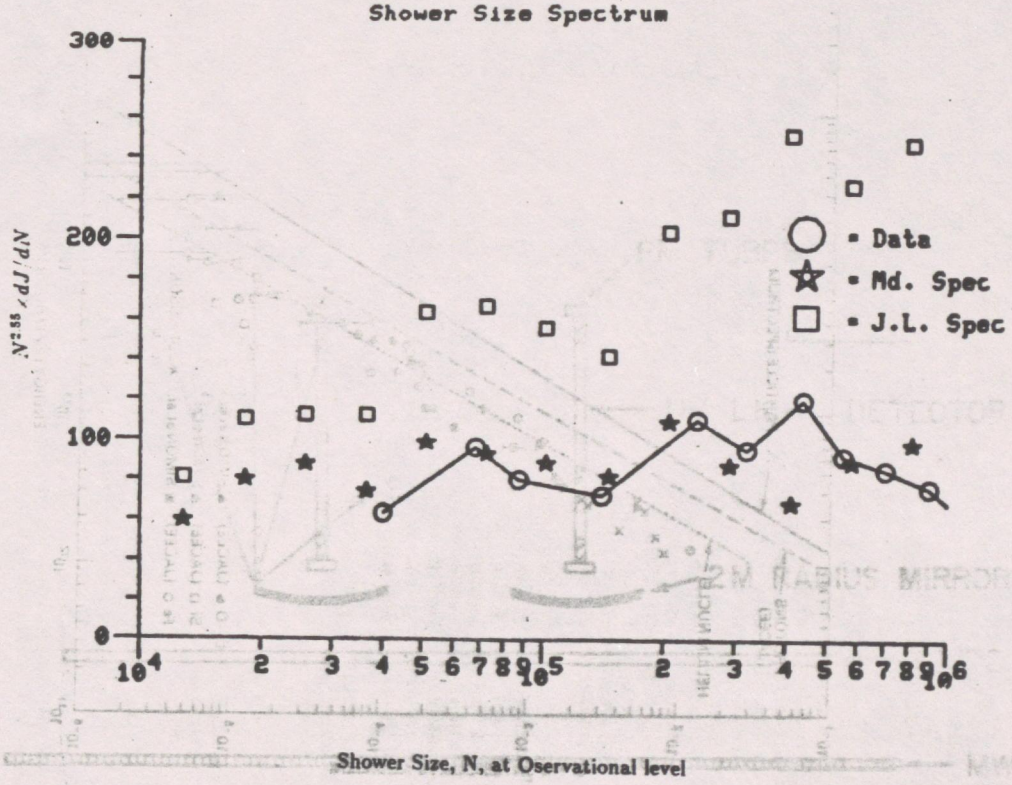
Shower Size Spectrum
• Data
• Md. Spec
• J.L. Spec
N^2.5 dJ/dN
Shower Size, N, at Oservational level

61-9

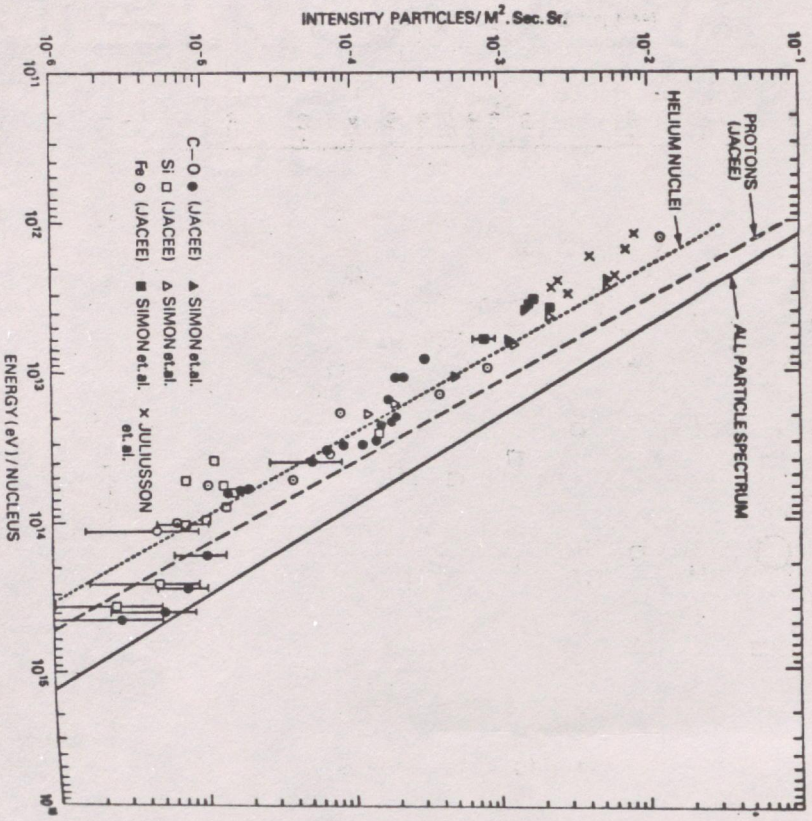

6-20

SCHEMATIC OF PROPOSED EXPERIMENT

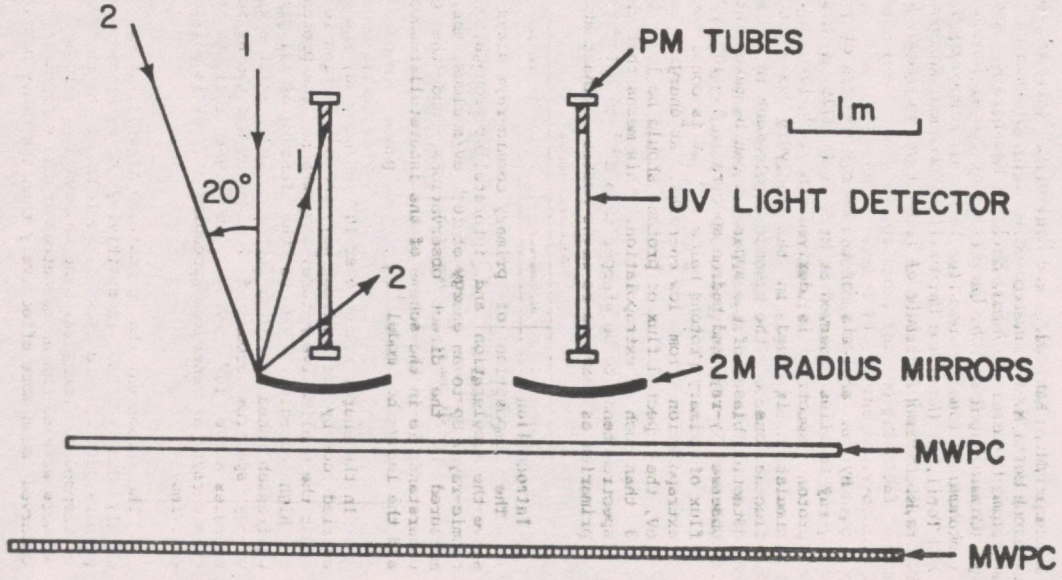

6-21